International Journal of Mass Spectrometry 307 (2011) 232–239

Contents lists available at ScienceDirect

International Journal of Mass Spectrometry

journal homepage: www.elsevier.com/locate/ijms

IMAGENA: Image Generation and Analysis – An interactive software tool handling LA-ICP-MS data

Tobias Osterholt[a], Dagmar Salber[a], Andreas Matusch[b], J. Sabine Becker[c], Christoph Palm[d,*]

[a] Institute of Neuroscience and Medicine (INM-1, INM-4), Research Centre Jülich, Germany
[b] Department of Psychiatry, University of Bonn, 53105 Bonn, Germany
[c] BrainMet Competence Centre, Central Division of Analytical Chemistry, Research Centre Jülich, Germany
[d] Faculty of Computer Science and Mathematics, Regensburg University of Applied Sciences, 93053 Regensburg, Germany

ARTICLE INFO

Article history:
Received 30 November 2010
Received in revised form 25 March 2011
Accepted 28 March 2011
Available online 23 April 2011

Keywords:
LA-ICP-MS
Image generation
Image analysis
Graphical user interface

ABSTRACT

Metals are involved in many processes of life. They are needed for enzymatic reactions, are involved in healthy processes but also yield diseases if the metal homeostasis is disordered. Therefore, the interest to assess the spatial distribution of metals is rising in biomedical science. Imaging metal (and non-metal) isotopes by laser ablation mass spectrometry with inductively coupled plasma (LA-ICP-MS) requires a special software solution to process raw data obtained by scanning a sample line-by-line. As no software ready to use was available we developed an interactive software tool for Image Generation and Analysis (IMAGENA). Unless optimised for LA-ICP-MS, IMAGENA can handle other raw data as well. The general purpose was to reconstruct images from a continuous list of raw data points, to visualise these images, and to convert them into a commonly readable image file format that can be further analysed by standard image analysis software. The generation of the image starts with loading a text file that holds a data column of every measured isotope. Specifying general spatial domain settings like the data offset and the image dimensions is done by the user getting a direct feedback by means of a preview image. IMAGENA provides tools for calibration and to correct for a signal drift in the *y*-direction. Images are visualised in greyscale as well a pseudo-colours with possibilities for contrast enhancement. Image analysis is performed in terms of smoothed line plots in row and column direction.

1. Introduction

Laser ablation inductively coupled plasma mass spectrometry (LA-ICP-MS) – introduced in 1980 by Houk and co-workers [1] – is today the most important and frequently used inorganic mass spectrometric technique which allows the direct analysis of solid samples without time-consuming sample preparation. LA-ICP-MS has been used for fast and precise in situ spatial resolved micro-local measurements of major, minor, and trace elements as well as isotope ratios with high analytical throughput applied in geology including age dating, in forensics, nuclear, environmental and material research [2]. Until recently, LA-ICP-MS has mainly been used in a line scan mode. Thus profiles of element distributions across samples constituted of parallel layers were obtained. A fascinating extension of LA-ICP-MS that emerged in the recent five years was the development of novel imaging techniques that permit the generation of quantitative maps of metal and non-metal distribution of sample surfaces, especially relevant to biomedical tissue sections [3].

In current instrumental settings of LA-ICP-MS based on commercial laser ablation systems the focused laser beam is at fix position and an ablation chamber with transparent cover glass containing the sample is placed on a *xyz*-stage. The sample is moved into the focus plain and a line by line ablation is realised by continuous motion in *x*-direction and a discontinuous motion in *y*-direction. At each line shift *x*-position is returned to zero while the laser is interrupted. As sample material is continuously transported to the mass spectrometer and the mass spectrometer operates continuously independent from the ablation system there is no trigger signal indicating a line shift. The number of data points acquired thus only depends from the total analysis time and the cycle time of the mass spectrometer needed for recording one mass spectrum. The primary output data is a continuous list of ion intensities. It is a certain challenge to determine the length of lines and to arrange these lines to a two dimensional image, which is further complicated by a dimension and interpolation problem in *y*-direction when the distance between lines exceeds the spot diameter permitting residual tissue between lines. Recently, a simulation software tool was introduced in order to assist optimisation of these ablation

* Corresponding author. Tel: +49 941 943 1314; fax: +49 941 943 1264
E-mail address: christoph.palm@web.de (C. Palm).
URL: http://www.chripa.de/AtWork (C. Palm).

1387-3806/$ – see front matter © 2011 Elsevier B.V. All rights reserved.
doi:10.1016/j.ijms.2011.03.010

parameters [4]. However, a precisely constant scan speed of the *xyz*-stage is the indispensable prerequisite for successful image reconstructions. Another challenge of software solutions is the correction for *y*-drifts that occur occasionally in single datasets in daily routine when the washing time of the ablation chamber and the equilibration time of the system were too short or during long lasting measurements i.e. over 14 h.

So far no commercial software is available to generate images from LA-ICP-MS data in a commonly readable parametric image file format. In an early phase images were reconstructed in a time consuming semi-manual manner using Matlab routines [5]. Recently this bottleneck in the process of LA-ICP-MS image acquisition has been closed by a C++ based software that is presented in this article. Formerly referred to as LA-ICP-MS-ImageGeneration [3,6–9] this software is now engagingly termed IMAGENA by this inaugural presentation. IMAGENA creates 8-bit greyscale TIFF-files that can be further treated with a plenty of freely or commercially available image analysis software. Calibration yielding parametric maps the pixel grey values of which equal the concentration at the pixel can either be performed on the level of IMAGENA or at a later stage. Calibration curves were mostly obtained by ablating a set of sections through homogenates spiked with known amounts of elements of interest in the line scan mode placed beside the sample in the same run [6,8–12]. Alternatively, homogenates were moulded into bores within the embedding medium before cryo-sectioning or solution based calibration was established [13]. Further treatment steps include co-registration to images of other modalities such as optical images, scaling, smoothing, and a read-out of average signals within free-hand drawn regions of interest (ROIs) such as the glass or blank background outside the sample and parcels based on anatomical criteria inside. The third dimension is accessible by LA-ICP-MS analysis of a set of serial sections covering the entire 3D object which is subject of forthcoming projects.

The sample used for demonstrative purposes in this paper was a 30 μm native cryo-section of a rat brain. A photothrombosis (PT) was induced 14 d before victimisation on the right frontal cortex according to the method of Watson et al. [14]. PT is assumed to model stroke. This type of sample has the advantage of a healthy hemisphere as internal comparator for the lesioned hemisphere. A high symmetry of non lesioned areas and the corpus callosum as reference structure with homogeneous element concentrations spanning across the major part of the *x* and *y* space allows to control for *x*- and *y*-signal drifts. A number of fine layers of different thickness and element concentrations allow an estimate of spatial resolution. Therefore, this sample can be seen as natural phantome for testing the performance of IMAGENA.

Past and current studies using quantitative LA-ICP-MS have been directed on the validation of animal models of stroke [7,15,16], tumours [3] Parkinsons [8] and Alzheimer disease [17], the study of human material [5,12] distribution studies of metallo-drugs [13] and toxic metals [10] in rodents, ex vivo calibration of in vivo imaging methods, optimisation of environmental monitoring using reporter organisms like molluscs [11,18] and plants [19]. Cerebral and other metallo-architecture has been assessed in humans [5,12], adult rodents [8] and during aging of rodents [6,20].

2. Materials and methods

2.1. Measurement setup

Bioimaging LA-ICP-MS measurements were performed using a quadrupole-based ICP-MS (Agilent 7500 ce) operated at a rf power of 1500 W, a carrier gas (argon) flow of 1.2 L min^{-1}. At a dwell time of 0.1 s per *m*/*z* the time expended for recording one mass spectrum composed of 26 selected *m*/*z* was 2.6 s. ICP-MS was coupled to a commercial laser ablation system (UP 266 from NewWave) with a focused laser beam (wavelength 266 nm, diameter of laser crater 120 μm and laser power density 3×10^9 W cm^{-2}, output energy 50%, scan speed 30 μm/s, distance between lines 150 μm). The ion intensities of metals of interest like zinc, copper and iron were measured by LA-ICP-MS within the ablated area. The example of this work bases on native rat brain cryo-sections with a tissue thickness of 30 μm that were scanned line-by-line. A photothrombosis according to the Watson model [14] was induced on the right frontal cortex 14 d before victimisation.

Table 1
Example of file content resulting from LA-ICP-MS measurements. The header is not shown.

Time [s]	C13	N15	O17	...
1353	84714	3623088	8596672	...
2696	82421	3559748	8609128	...
4039	79283	3448909	8539204	...
5383	88518	3761866	8709733	...
...	...	...	...	...

2.2. Image Generation and Analysis Software

The software *Ima* ge *Gen* eration and *A* nalysis (IMAGENA) was optimised for speeding up post-processing of LA-ICP-MS data and allows high-throughput analysis providing an easy-to-use graphical user interface (Fig. 1). The process of visualisation and analysis of LA-IPC-MS data consists of four main steps:

- Adjustment of the spatial domain,
- Calibration,
- Contrast enhancement,
- Measurement analysis.

2.2.1. Adjustment of the spatial domain

In general, the raw data of the LA-ICP-MS measurements are stored in a file starting with header information followed by the measurement results of each isotope in column order. Additionally, the first column contains the time stamp of the measurements (Table 1).

The spatial domain is determined by the image width and height as well as the spacing, i.e. the size of each pixel. The spacing in the *x*-direction directly depends on the time needed for the acquisition of a single mass spectrum t_{aq} including a reset time and the table *x*-propagation speed v. The number n of data points obtained on a line of the length l will be $n = l \cdot v^{-1} \cdot t_{aq}^{-1}$. The spacing in the *y*-direction depends on the chosen distance between the lines.

Laser scanning was done line by line. However, the data output of the LA-ICP-MS system is streamed continuously yielding non-tissue measurement values at the beginning of each file. Keeping the laser at a fixed position, the first line scan is started when the sample table starts moving. This very first scan line measurement is not labeled in the measurement file and cannot be detected by a significant increase of measurement values, because in general tissue has arbitrary shape and does not cover the upper left corner of the scanning field. This gives reason for the necessity of an user defined *offset* cutting out the non-tissue values recorded before the first line scan has started.

Each line scan lasts a user defined period. This period defines inherently the number of measurements per line given the time needed for acquisition of one mass spectrum. However, in general the line scanning period is not an integer multiple of the scanning time per measurement. That means, that the number of measurements per line may vary plus-minus one.

IMAGENA adjusts for this variation allowing the user to define *floating point width* values. Because all lines have to be of the same length to result in a valid image and because there are no fractional

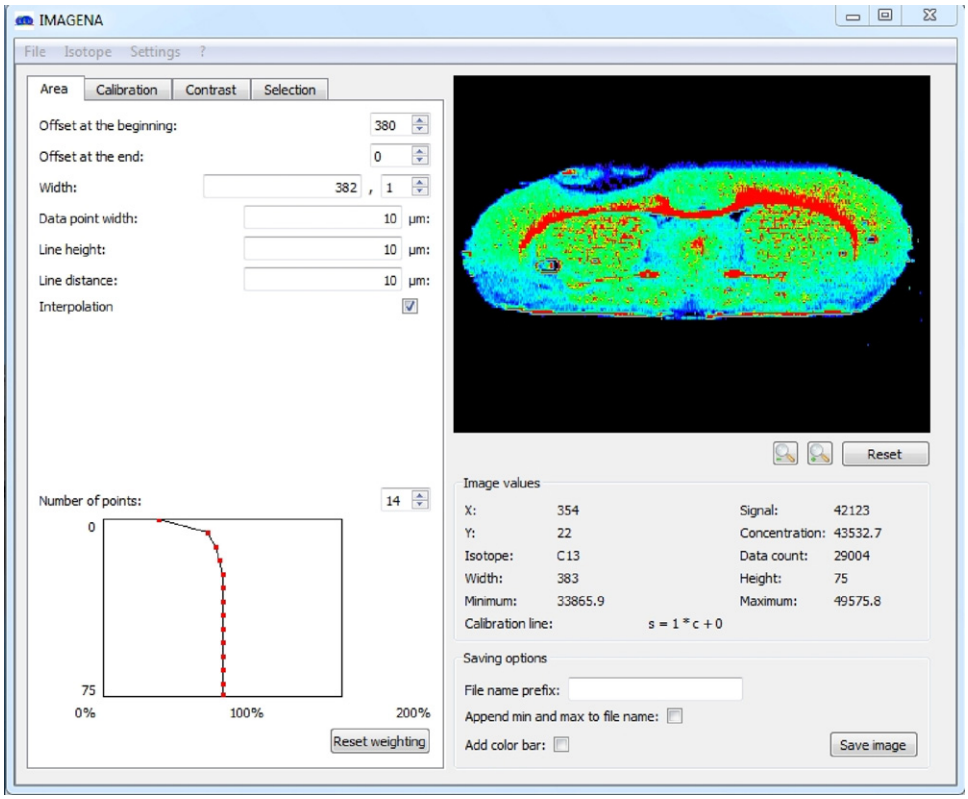

Fig. 1. Graphical user interface of IMAGENA.

0	1	2	2	0+0.6=0.6 <1
3	4	5	6	0.6+0.6=1.2 >1
7	8	9	9	1.2−1+0.6=0.8 <1
10	11	12	13	0.8+0.6=1.4 >1

Fig. 2. Example of floating point width 3.6. The numbers in the image matrix on the left indicate the measurement index of the scanning file. The fcv is shown on the right.

pixels possible, each line consists of the integer part of the width plus one. The last pixel of a row is filled either with the next value of the measurement column or by duplicating the current value. To decide on this, the fraction control value (fcv) is introduced here. The fcv of row r for a width fraction f is defined as follows:

$$\mathrm{fcv}(r) = \begin{cases} 0 & \text{if} \quad r < 0 \\ \mathrm{fcv}(r-1) + f & \text{if} \quad \mathrm{fcv}(r-1) < 1 \text{ AND } r \geq 0 \\ \mathrm{fcv}(r-1) + f - 1 & \text{if} \quad \mathrm{fcv}(r-1) \geq 1 \text{ AND } r \geq 0 \end{cases} \tag{1}$$

Fig. 2 illustrates the principle of line length variation due to the fcv.

In order to reduce the overall scanning time and to avoid undermining and detachment of the residual tissue flap from the glass surface usually the distance between lines is chosen greater than the laser spot diameter. IMAGENA allows the user to specify the line height, and the distance between lines which corresponds to the height of the residual tissue-bars between ablated lines in steps of 10 µm. The pixel height is set to the largest common numerator of both parameters. IMAGENA fills the left-out lines with values interpolated from the pixels above and below. For this, the mean value of the adjacent measurements are computed (Fig. 3).

2.2.2. Calibration

Calibration is an important issue to come to quantitative analysis of the spatial isotope distribution and to allow comparability of distributions of different individuals. For calibration the functional dependency of the signal, which is the measured ion intensity, and the element concentration has to be estimated. Linear calibration curves are based on the measurement of prepared laboratory standards of defined added element concentrations. In our experiments, laboratory standards with rising concentrations of zinc, copper and iron were used [6]. Within IMAGENA a linear regression through an arbitrary number N of pairs of signal and added concentration (s_n, c_n) is carried out, yielding a straight line of the form

$$s = a \cdot c + b \tag{2}$$

with

$$a = \frac{\sum_{n=1}^{N} c_n \cdot s_n - N \cdot \bar{c} \cdot \bar{s}}{\sum_{n=1}^{N} c_n^2 - N \cdot \bar{c}^2} \tag{3}$$

7	2	5	5	6	3	2
0	0	0	0	0	0	0
9	2	4	6	7	5	3

7	2	5	5	6	3	2
8	2	4	5	6	4	2
9	2	4	6	7	5	3

Fig. 3. Interpolation. Left-out lines are filled with zero (left) and optionally substituted by values computed due to a column-based interpolation (right). The numbers represent measurement and interpolated values.

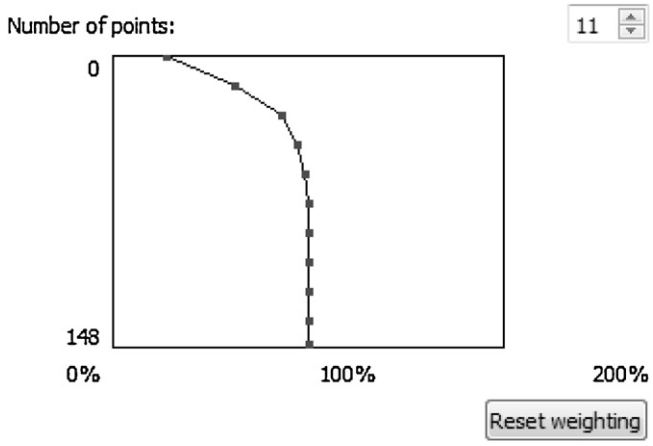

Fig. 4. Correction function. Piecewise linear weighting function in dependency of the number of the laser scanning line. The dots depict the anchor points for manual function definition.

given

$$\bar{c} = \frac{1}{N}\sum_{n=1}^{N} c_n \quad \text{and} \quad \bar{s} = \frac{1}{N}\sum_{n=1}^{N} s_n \tag{4}$$

Then, the total element concentration in the sample g is calculated as follows:

$$g = \frac{s - B_g}{a} \tag{5}$$

with glass background B_g measured around the sample-slice determined in an exported raw TIFF-image using standard image analysis software.

Exceptionally, images obtained by LA-ICP-MS may present a signal drift in the y-direction. IMAGENA provides tools to correct for these y-drifts. Other than by visual inspection a y-drift can be noticed by plotting the measurement values of non-tissue (background) measurements orthogonal to the laser scanning lines. Considering the laser scanning lines as rows of an image, the orthogonal lines are the image columns. A background column has to be constant except for system specific noise. IMAGENA provides a plotting tool not only for image columns but also for image rows as part of the image analysis functionality (Section 2.2.4). If a bias is detected, the values of each scanning line are corrected using a weighting function depending on the number of the line scan, i.e. for each line a constant weighting factor is determined.

The weighting function is piecewise linear with anchor points specifying the points of intersection of adjacent linear functional pieces. The weighting factors range between 0 and 2. The number of pieces of this function as well as the value of the anchor points are determined manually. Be s_{uv} the uth measurement value on line v and $w(v)$ the weighting factor of row v. Then, the corrected measurement s'_{uv} is computed by

$$s'_{uv} = w(v) \cdot s_{uv} \quad \text{for all } u \tag{6}$$

Fig. 4 shows an example of the weighting function.

2.2.3. Contrast enhancement

After specification of the spatial domain and optional calibration, the LA-ICP-MS data are transformed into a two-dimensional (2D) greyscale image, where intensities correspond to measurement values. To focus on structures of interest, to suppress noise in background regions and to correct for artificial single value outliers with extremely high signal, the intensities are normalised using a piecewise linear contrast enhancement function. Considering a

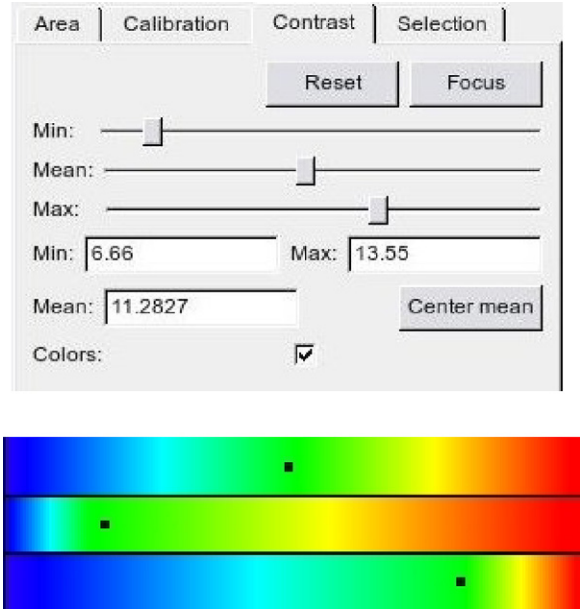

Fig. 5. Pseudo-colouring. Top: Graphical user interface for contrast enhancement. Bottom: The standard colour scale (top row) is modified by moving the mean colour in the direction of blue (middle row) or in the direction of red (bottom row). (For interpretation of the references to colour in this figure legend, the reader is referred to the web version of the article.)

maximum grey value G and a user defined minimum and maximum value, min and max, respectively (Fig. 5, top). Then, the grey value g' in the enhanced image is computed given the original grey value g as follows:

$$g' = \begin{cases} 0 & \text{if} \quad g < \min \\ G & \text{if} \quad g > \max \\ G \cdot \dfrac{g - \min}{\max - \min} & \text{else} \end{cases} \tag{7}$$

Additionally, contrast enhancement is based on pseudo-colouring of the greyscale image. Pseudo-colouring means, that each intensity is mapped to a colour consisting of red, green and blue component. Colours help to distinguish between low contrast structures and to visualise high signal peaks. To support this, the colours are chosen according to the hue circle of the hue-saturation-value (HSV) colour space with a modification in the green part. The human visual system has deficiencies in discrimination of similar green colours. This resulted in the development of the *Luv* colour space which is perceptually uniform [21]. Similarly, we corrected the hue circle by reducing the green part to weight all colour regions equally. Blue indicate low intensities, green medium and red high intensities. Zero intensity is mapped to black.

In the pseudo-colour mode of IMAGENA, not only the minimum and the maximum value is adaptable but also the colour mean placed in the green part of the hue circle. Moving the colour mean to the left in the direction of blue, the blue colours are packed and the yellow and red colours are spread. Moving the colour mean to the right in the direction of red, yellow and red are packed and blue is spread (Fig. 5, bottom). The colour scale chosen for an image is optionally integrated directly as lower part of the image for documentation.

2.2.4. Measurement analysis

The image analysis functionality of IMAGENA focuses on scan line plotting and mean computation of high signal areas. A scan line plot is done for image rows, i.e. in the direction of the laser scanning, and for image columns. To avoid noisy plots, at each plot

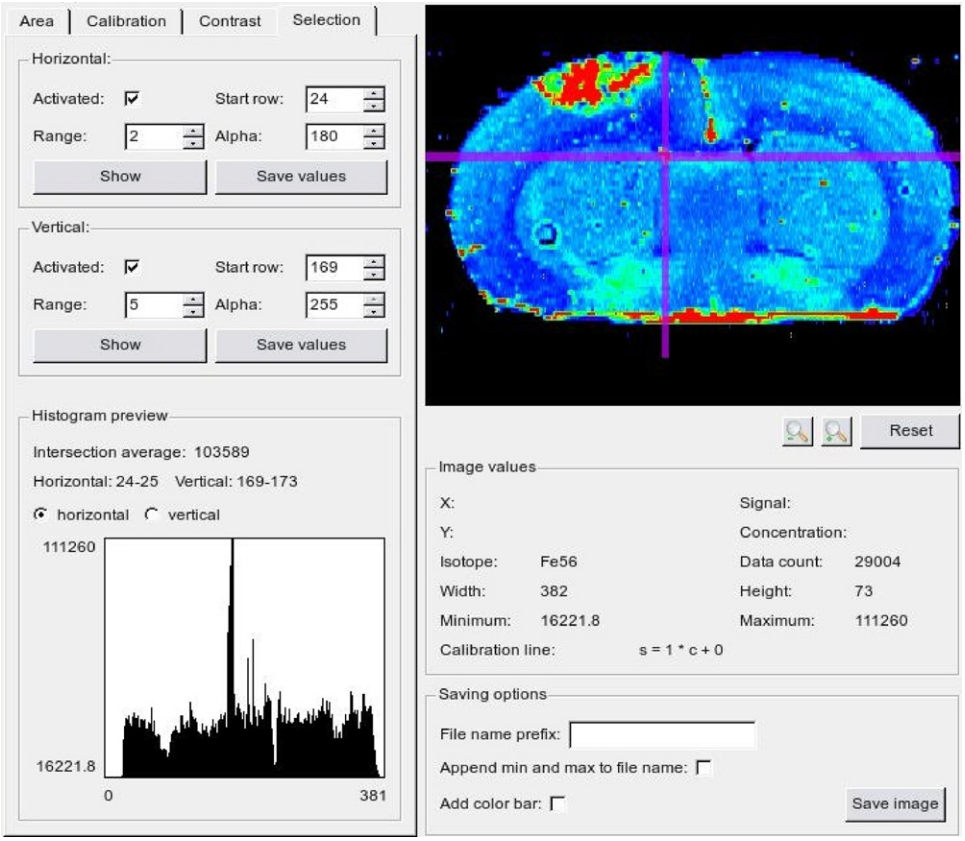

Fig. 6. Line plot. Graphical user interface of IMAGENA showing the selection of 5 rows and 5 columns intersecting in a 5 × 5 rectangular region of interest. The selected plot areas are labeled by magenta lines in the image in the upper right corner. In the lower left corner, the horizontal line plot is shown. (For interpretation of the references to colour in this figure legend, the reader is referred to the web version of the article.)

position the mean value of a user defined number of rows/columns is chosen instead of a single line plot.

The position of the line plot in the image is interactively chosen. Additional to a plot preview within the graphical user interface of IMAGENA, the plot values can be saved in a textfile to allow post-processing with external plot software. Row plot area and column plot area intersect and mark a rectangular region of interest. IMAGENA provides the mean value of the measurements within this area. This tool is especially useful to analyse high intensity spots (Fig. 6).

2.3. Implementation details

IMAGENA was implemented using C++ combined with a Qt graphical user interface [22]. Platform independent software development allows the compilation on windows, linux and MacOS system software. IMAGENA was build up in a modular architecture to simplify further functionality extensions. Images are generated following a pipelining principle starting with data import and spatial domain specifications followed by the application of calibration procedures and contrast enhancement and ending with the visualisation and result storage. In memory both are hold, the raw data as well as the image data which are user specific adapted and visualised. Depending on the changes made during the IMAGENA session, only those parts of the pipeline are updated and repeatedly computed which are necessary for a correct result. This saves computation time and results in high stability of the software.

To ease the working with IMAGENA some helpful little features were implemented. One feature is the possible storage of a log-file which helps to reconstruct all generation and analysis steps done for a specific image. Additionally a profile is storable which allows the specification of some parameters which do not change from session to session. Loading the profile at the beginning allows the efficient start of the IMAGENA session without need of repeated parameter input. Which parameters are stored in the profile is user selectable.

The storage of resulting images is simplified by a predefined file name starting with the label of the isotope chosen. This predefined name is accompanied by a user defined prefix to extend the file name by the current date and/or study name. This prefix is constant for the whole IMAGENA session and speeds up the image storage process. The resulting images are stored in uncompressed tif-format optionally extended by the greyscale or colour scale used.

3. Results

IMAGENA has been used on a daily base in the BrainMet competence centre and was able to reduce the time for Image Generation and Analysis significantly. Results of the software were already basis for publications [3,6,8,16]. It is easy to use and has a self-explaining user interface. Although it was optimised for LA-ICP-MS data it is adaptable to handle all kinds of column-related raw data which should be converted to a 2D image. In the following, some results using specific IMAGENA features are given in detail.

The offset determines the starting point of the first scanning line in the data file. Wrong offset values result in a split sample. The connectivity of the sample is given wrap-around continuing the image at the left hand side with the image part on the right hand side. Therefore, the correct offset is specified, if the whole sample appears as a connected object. Fig. 7 shows the effect of increasing offset value. In the first image for offset 0 just one column

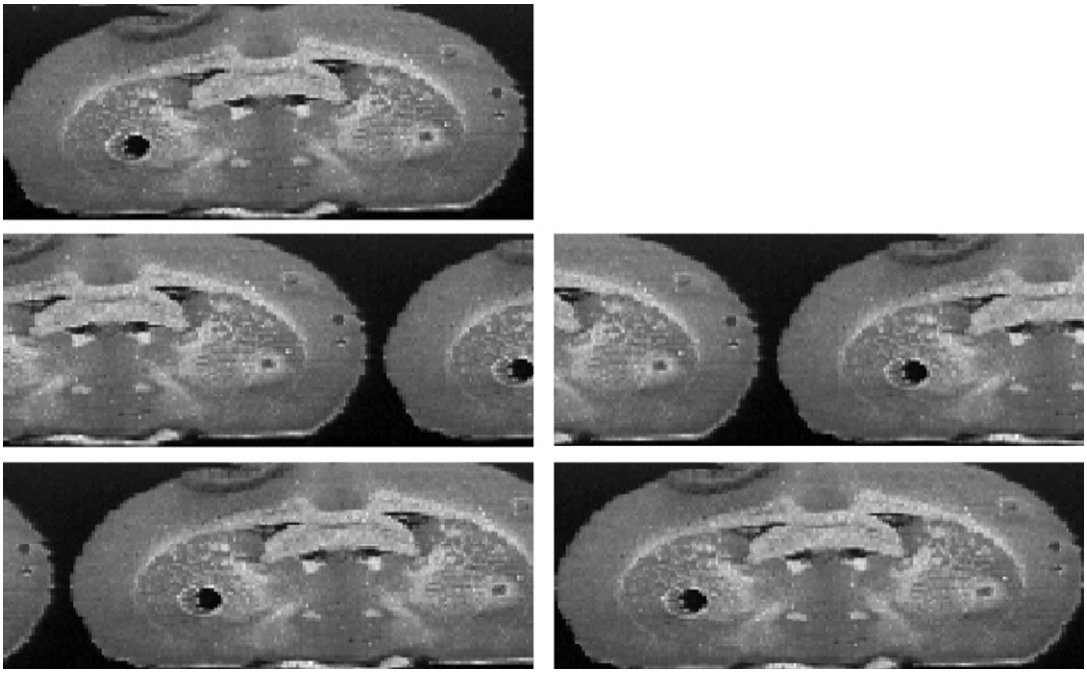

Fig. 7. Offset variation. Starting from offset 0, the offset is increased in steps of 40.

is split from the sample. Therefore, nearly the complete first row has to be cut by the offset. Increasing offset resulted in a move of the sample appearance to the left, coming wrap-around back on the right.

IMAGENA allows the specification of a non-integer image width to consider the effect of a fixed line scanning period and a non-matching scanning time per measurement. Without the fractional part of the width the sample may appear sheared (Fig. 8). The correction was done taking the histologic appearance of the sample into account.

The correction of signal drift in the *y*-direction using a weighting function is visualised in Fig. 9. The column line plot of the background based on the magenta labeled area within the pseudo-coloured image showed significantly higher measurement values for the first few scanning lines. Using the weighting function with 15 anchor points shown on the right in the bottom row, the bias was reduced. In the resulting column line plot only unbiased noise remain.

Fig. 10 is meant to illustrate the effect of calibration and contrast enhancement. The left image is not calibrated. Additionally, one signal outlier (labeled with red circle) shows a significantly higher value than all other measurements. Beside the signal spot nearly no other sample parts can be observed. Only after calibration with the help of an estimated linear function and a user defined max value the structures of the sample become visible (right image).

Pseudo-colouring helps to visualise the isotope distribution and to focus on tissue parts with varying concentrations. Fig. 11 shows four images of the same isotope distribution with different min-, mean-, and max-values. The first row focus on the effect of changing min and max values. The left image shows low contrast with hardly distinguishable inner structures of the tissue sample. The bluish background traces back to the fact, that system noise remain in non-tissue measurements. The image on the right was optimised due to high contrast and noise level reduction. The background is homogeneously black by taking a user defined min value above the noise values into account. The intensity differences of the inner structures are now clearly visible by reducing the max value. In both images of the top row the mean value keeps in the middle between min and max value.

The bottom row shows the effect of mean value variation. Starting point for min and max value is their position in Fig. 11 (top, right). The mean value was moved to the right reducing red and yellow and broadening the blue colours and was respectively moved to the left reducing blue and show a wide range of yellow and red resulting in the left and right image. See Fig. 5 for an explanation of the colour scales.

4. Discussion

IMAGENA is able to handle LA-ICP-MS data, generate calibrated images with high contrast, is able to deal with common problems like signal outliers and drifts in the *y*-direction, provides tools for row and column line plotting and enables easy image storage. IMAGENA is not only a proof of concept but is already in routine use.

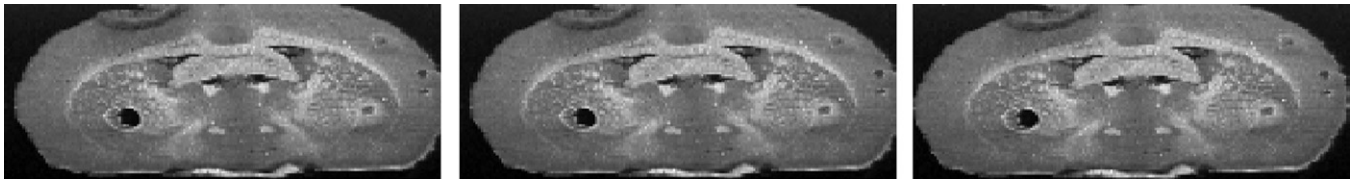

Fig. 8. Result of fractional width. Starting from fraction 0 (left), the fractional part is increased to 1 (middle) and 2 (right). The image of the sample, a coronal rat brain section, is less (left) or more (right) centred in the rectangular image screen.

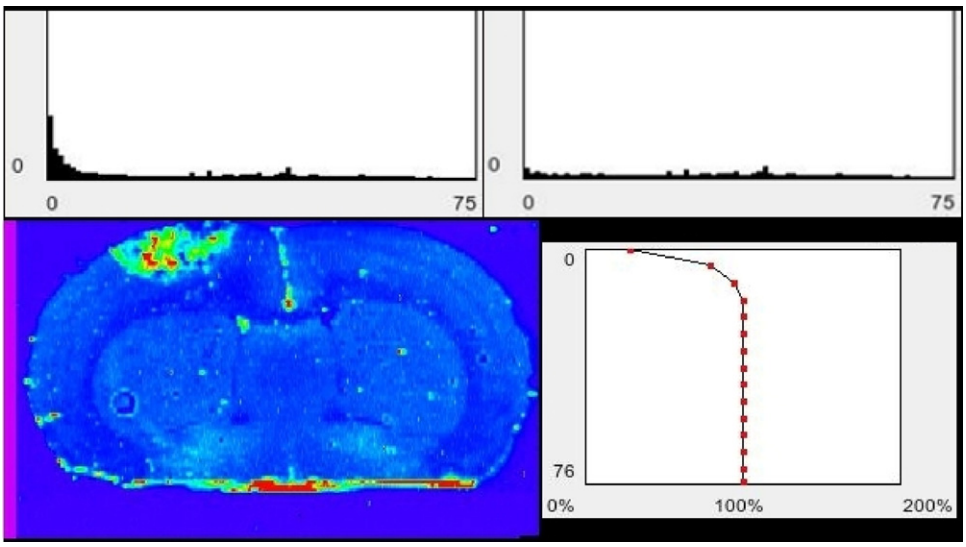

Fig. 9. Correction of drift in the *y*-direction. Top row: Column line plot before (left) and after (right) correction of drift in the *y*-direction. Bottom row: The pseudo-coloured image is shown with the background area as basis for the column line plots labeled in magenta (left). The weighting function used for correcting the drift (right). (For interpretation of the references to colour in this figure legend, the reader is referred to the web version of the article.)

All features of IMAGENA were requested by practitioners and were implemented in close contact with the users. After a first prototype the current release is a re-implementation with tidy graphical user interface and improved stability.

IMAGENA was developed as an interactive tool although manual parameter setting means user dependency and, thus, may yield lacks in reproducibility. Especially the parameters to determine the spatial domain like offset and width fraction should be user independent. Some additional measures in the setup of LA-ICP-MS may help to determine these parameters without user interaction. For example, applying a straight line with defined isotope concentration on the glass slide beside the sample may help to determine the offset as well as the width fraction. However, such a line has to be very thin and should be exactly orthogonal to the laser scanning line. These preconditions are hardly realisable.

A second idea is based on a shape reference by using a microphotograph of the section taken before laser ablation. Those images can be registered affinely to the image of isotope distribution [23] following an adequate registration strategy for section images [24]. The spatial domain parameters can be optimised during the iterative registration procedure. However, in general registration does not yield a unique result due to local optima.

In the ideal case the ablation area should be greater than the sample or standard tissue slice so that the sample is surrounded by glass background in order to

1. facilitate shape recognition and reconstruction,
2. to allow correct measurement and subtraction of glass background,
3. to allow *y*-drift correction.

IMAGENA only covers the special case of unidirectional ablation in a set of parallel lines. In order to minimize secondary aerosol deposition onto un-ablated areas of the sample movement of the sample desk into the same direction as the carrier gas stream proved obligatory. Scanning the lines in alternating direction (Meander-like pattern) also orthogonally to the carrier gas stream was tested in our laboratory but lead to alternating *x*-drifts.

In case of unidirectional ablation, spatial domain parameters are easy to optimise using the visual feedback of IMAGENA. The split effect of a wrong offset as well as the shearing effect of a wrong width fraction can easily be observed and corrected. Differing parameter determinations of different users were never observed and hardly possible.

The contrast enhancement, interpolation, pseudo-colouring and calibration tools give the user possibilities to change the visual appearance of the isotope distribution. This is necessary to correct for disturbing effects and to focus on isotope differences otherwise not detectable although existent. IMAGENA allows the storage of a log file for documentation of the processing steps. Additionally, the default filenames contain the most important parameters like user defined min and max values. This helps to interpret the resulting images appropriately.

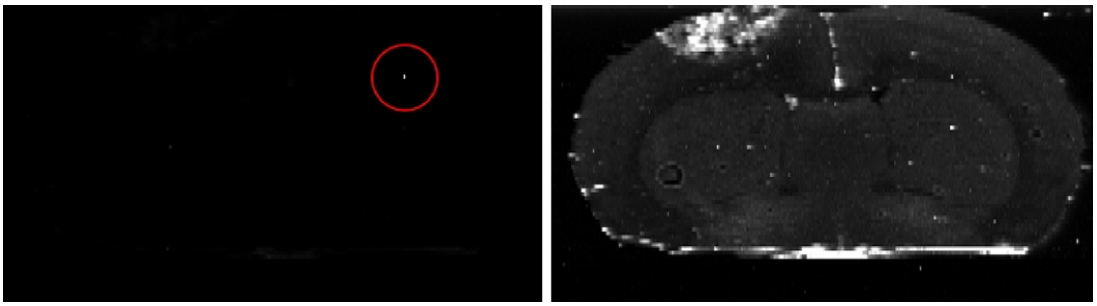

Fig. 10. Calibration and contrast enhancement. The uncalibrated image (left) shows one intensity outlier, which is marked with a red circle. The right image is calibrated with a linear function and contrast enhanced with a user defined max value. (For interpretation of the references to colour in this figure legend, the reader is referred to the web version of the article.)

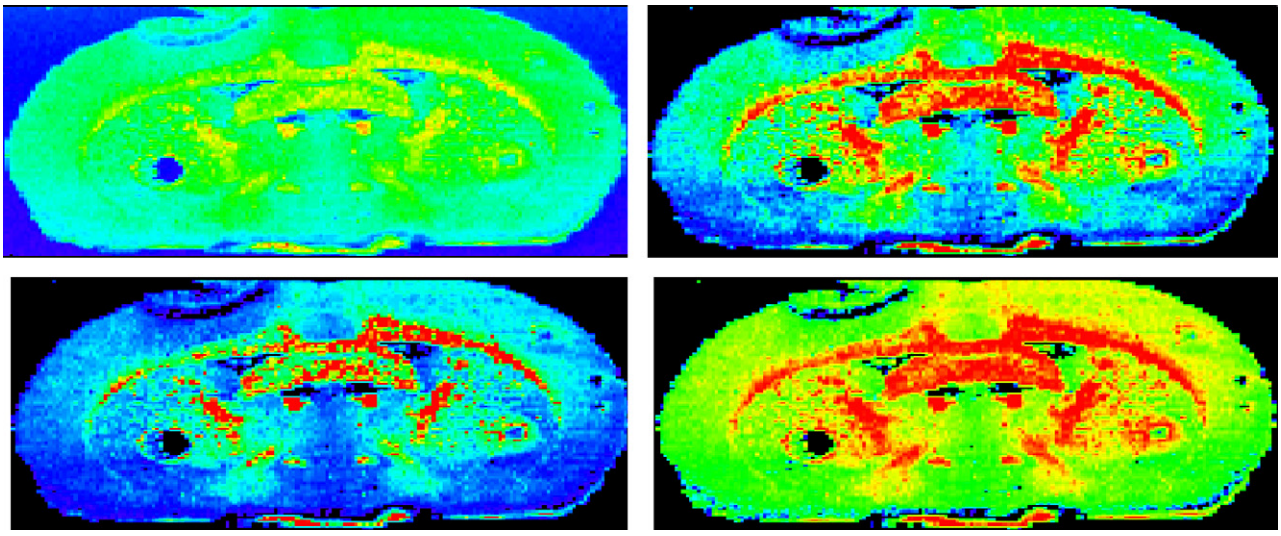

Fig. 11. Result of pseudo-colouring. Top row: Data driven max and min values (left) and user optimised max and min values (right). In both images the mean value halves the range of min and max. Bottom row: Starting from user defined min and max values, the mean value is moved in the direction of red (left) and in the direction of blue (right) on the hue circle.

5. Conclusion

IMAGENA is a versatile and valuable tool to reconstruct images from the continuous stream of raw data resulting from LA-ICP-MS imaging experiments. Images can be visualised, corrected, levelled out, calibrated and converted into TIFF-files that can be further treated with standard image analysis software. IMAGENA proved its suitability and usefulness in more than two years of routine use. IMAGENA closed a significant bottleneck in the process of LA-ICP-MS image generation.

References

[1] R.S. Houk, V.A. Fassel, G.D. Flesch, H.J. Svec, A.L. Gray, C.E. Taylor, Inductively coupled argon plasma as an ion-source for mass-spectrometric determination of trace-elements, Anal. Chem. 52 (1980) 2283–2289.

[2] J.S. Becker, Inorganic Mass Spectrometry: Principles and Applications, John Wiley and Sons, Chichester, 2007.

[3] J.S. Becker, M. Zoriy, A. Matusch, B. Wu, D. Salber, C. Palm, Bioimaging of metals by laser ablation inductively coupled plasma mass spectrometry (LA-ICP-MS), Mass Spectrom. Rev. 29 (2010) 156–175.

[4] J. Triglav, J.T. van Elteren, V.S. Selih, Basic modeling approach to optimise elemental imaging by laser ablation ICPMS, Anal. Chem. 82 (2010) 8153–8160.

[5] J.S. Becker, M.V. Zoriy, C. Pickhardt, N. Palomero-Gallagher, K. Zilles, Imaging of copper, zinc, and other elements in thin section of human brain samples (hippocampus) by laser ablation inductively coupled plasma mass spectrometry, Anal. Chem. 77 (2005) 3208–3216.

[6] J.S. Becker, A. Matusch, C. Palm, D. Salber, K.A. Morton, S. Becker, Bioimaging of metals in brain tissue by laser ablation inductively coupled plasma mass spectrometry (LA-ICP-MS) and metallomics, Metallomics 2 (2010) 104–111.

[7] J.S. Becker, D. Salber, New mass spectrometric tools in brain research, Trends Anal. Chem. 29 (2010) 966–979.

[8] A. Matusch, C. Depboylu, C. Palm, B. Wu, G.U. Hoglinger, M.K. Schafer, J.S. Becker, Cerebral bioimaging of Cu, Fe, Zn, and Mn in the MPTP mouse model of Parkinson's disease using laser ablation inductively coupled plasma mass spectrometry (LA-ICP-MS), J. Am. Soc. Mass Spectrom. 21 (2010) 161–171.

[9] J.S. Becker, U. Breuer, H.F. Hsieh, T. Osterholt, U. Kumtabtim, B. Wu, A. Matusch, J.A. Caruso, Z. Qin, Bioimaging of metals and biomolecules in mouse heart by laser ablation inductively coupled plasma mass spectrometry and secondary ion mass spectrometry, Anal. Chem. 82 (2010) 9528–9533.

[10] J.S. Becker, J. Dobrowolska, M. Zoriy, A. Matusch, Imaging of uranium on rat brain sections using laser ablation inductively coupled plasma mass spectrometry: a new tool for the study of critical substructures affined to heavy metals in tissues, Rapid Commun. Mass Spectrom. 22 (2008) 2768–2772.

[11] J.S. Becker, A. Matusch, C. Depboylu, J. Dobrowolska, M.V. Zoriy, Quantitative imaging of selenium, copper, and zinc in thin sections of biological tissues (Slugs-Genus arion) measured by laser ablation inductively coupled of plasma mass spectrometry, Anal. Chem. 79 (2007) 6074–6080.

[12] J. Dobrowolska, M. Dehnhardt, A. Matusch, M. Zoriy, N. Palomero-Gallagher, P. Koscielniak, K. Zilles, J.S. Becker, Quantitative imaging of zinc, copper and lead in three distinct regions of the human brain by laser ablation inductively coupled plasma mass spectrometry, Talanta 74 (2008) 717–723.

[13] D. Pozebon, V.L. Dressler, M.F. Mesko, A. Matusch, J.S. Becker, Bioimaging of metals in thin mouse brain section by laser ablation inductively coupled plasma mass spectrometry: novel online quantification strategy using aqueous standards, J. Anal. At. Spectrom. 25 (2010) 1739–1744.

[14] B.D. Watson, W.D. Dietrich, R. Busto, M.S. Wachtel, M.D. Ginsberg, Induction of reproducible brain infarction by photochemically initiated thrombosis, Ann. Neurol. 17 (1985) 497–504.

[15] D. Salber, F. Uhlenbrock, J. Manuvelpillai, B. Wu, C. Palm, A. Matusch, K.J. Langen, J.S. Becker, Imaged by LA-ICP-MS: metal accumulations after cerebral infarct in course of time, FEBS J. 277 (2010) 83–84.

[16] D. Salber, J. Manuvelpillai, I. Spahn, S. Klein, F. Uhlenbrock, C. Palm, A. Matusch, S. Becker, K.J. Langen, H.H. Coenen, Ti-45-cations as potential PET tracers for cerebral neurodegeneration, Nucl. Med. Biol. 37 (2010) 726–1726.

[17] R.W. Hutchinson, A.G. Cox, C.W. McLeod, P.S. Marshall, A. Harper, E.L. Dawson, D.R. Howlett, Imaging and spatial distribution of beta-amyloid peptide and metal ions in Alzheimer's plaques by laser ablation-inductively coupled plasma-mass spectrometry, Anal. Biochem. 346 (2005) 225–233.

[18] D.S. Gholap, A. Izmer, B. De Samber, J.T. van Elteren, V.S. Selih, R. Evens, K. De Schamphelaere, C. Janssen, L. Balcaen, I. Lindemann, L. Vincze, F. Vanhaecke, Comparison of laser ablation-inductively coupled plasma-mass spectrometry and micro-X-ray fluorescence spectrometry for elemental imaging in Daphnia magna, Anal. Chim. Acta 664 (2010) 19–26.

[19] B. Wu, M. Zoriy, Y.X. Chen, J.S. Becker, Imaging of nutrient elements in the leaves of Elsholtzia splendens by laser ablation inductively coupled plasma mass spectrometry (LA-ICP-MS), Talanta 78 (2009) 132–137.

[20] L.M. Wang, J.S. Becker, Q. Wu, M.F. Oliveira, F.A. Bozza, A.L. Schwager, J.M. Hoffman, K.A. Morton, Bioimaging of copper alterations in the aging mouse brain by autoradiography, laser ablation inductively coupled plasma mass spectrometry and immunohistochemistry, Metallomics 2 (2010) 348–353.

[21] M. Tkalcic, J.F. Tasic, Colour spaces: perceptual, historical and applicational background, in: EUROCON 2003, vol. 1, 2003, pp. 304–308.

[22] qt.nokia.com.

[23] A. Matusch, A. Bauer, J.S. Becker, Element imaging in formalin fixed slices of human mesencephalon. Int. J. Mass Spectrom., in this issue.

[24] C. Palm, A. Vieten, D. Salber, U. Pietrzyk, Evaluation of registration strategies for multi-modality images of rat brain slices, Phys. Med. Biol. 54 (2009) 3269–3289.